# Element- and site-specific oxidation state and cation distribution in manganese ferrite films by diffraction anomalous fine structure

Aria Yang,[1,a)] Zhaohui Chen,[1] Anton L. Geiler,[1] Xu Zuo,[2] Daniel Haskel,[3] E. Kravtsov,[3] C. Vittoria,[1] and V. G. Harris[1]
[1]*Department of Electrical and Computer Engineering and the Center for Microwave Magnetic Materials and Integrated Circuits, Northeastern University, Boston, Massachusetts 02115, USA*
[2]*College of Information Technical Science, Nankai University, Tianjin 300071, People's Republic of China*
[3]*Advanced Photon Source, Argonne National Laboratory, Argonne, Illinois 60439, USA*

(Received 2 April 2008; accepted 9 July 2008; published online 8 August 2008)

Epitaxial manganese ferrite thin films were studied by x-ray diffraction anomalous fine structure to obtain element-specific and site-specific information on site occupancy, local structure, and valency. These properties were introduced to molecular field theory to reproduce thermomagnetization curves and determine superexchange energy, Néel temperature, and spin canting angle. © *2008 American Institute of Physics*. [DOI: 10.1063/1.2969406]

Spinel ferrites represent an important class of materials that provide high permeability, moderate to high permittivity, and low microwave loss for devices that send and receive electromagnetic signals. Such devices include monolithic microwave integrated circuits that find wide use in radar and wireless communication technologies. To enable ferrite compatibility with planar integrated circuit design, research emphasis has been placed on the preparation of ferrites as films. To this end, we have employed the alternating-target laser ablation deposition technique, where sequential ablation from multiple targets allows control of ion location within the unit cell.[1,2] This approach to ferrite film synthesis has resulted in materials having enhanced magnetization[2] and magnetic anisotropy fields.[1]

The spinel ferrite adopts a closed packed oxygen lattice where transition metal ions occupy eight tetragonal ($A$) sites and 16 octahedral ($B$) sites within one unit cell. Studies using extended x-ray absorption fine structure (EXAFS) analysis demonstrated the ability to quantify the element-specific cation distribution on tetrahedral and octahedral sites.[3–6] However, the site-specific and element-specific oxidation state of these ions, information that is critical in determining the superexchange interaction and other intrinsic magnetic properties, remained elusive. Here, we employ diffraction anomalous fine structure[7,8] (DAFS) to measure element-specific and site-specific information. We introduced this information to molecular field theory to determine the superexchange energy, Néel temperature, and spin canting angle in Mn-ferrite ($MnFe_2O_4$) films.

The Mn-ferrite film was deposited on a MgO (111) substrate in an oxygen pressure of 1 mTorr and 700 °C following a deposition sequence that included ten laser shots from a $Fe_2O_3$ target, followed by four shots from a MnO target with this sequence repeated 1000 times. The x-ray diffraction measurements confirmed the epitaxial growth in the manganese ferrite film. The Néel temperature was determined from thermomagnetization measurement from 4 to 675 K. The Mn-ferrite film sample was found to have a Néel temperature of 595 K, which is 22 K higher than the bulk value of 573 K.

The investigation of element-specific and site-specific short-range order and oxidation state was performed using DAFS. Data were collected using the 4-ID-D undulator beamline of the Advanced Photon Source at Argonne National Laboratory. The DAFS scans were carried out by scanning the x-ray energy through the Mn and Fe absorption edges while maintaining the sample's Bragg condition using a diffractometer. In order to apply absorption corrections to the DAFS signal, EXAFS spectra were collected simultaneously in fluorescence mode.

For the present study, the (422) and (222) Bragg reflections were selected to obtain element-specific local structure information for crystallographically inequivalent sites. An iterative Kramers–Krönig algorithm[9–11] was employed to reduce the measured DAFS spectra to EXAFS-like data. The accuracy of this approach was demonstrated through self-consistency checks of the derived EXAFS data.[10]

The EXAFS data were analyzed using the IFEFFIT-based suite of programs, ATHENA and ARTEMIS.[12] The model used in determining cation distribution in ferrite materials followed that of Harris and co-workers[3,4] and Calvin and co-workers.[5,6] The inversion parameter $\delta$, defined here as $(Mn_{1-\delta}Fe_{\delta})^{tet}[Mn_{\delta}Fe_{2-\delta}]^{oct}O_4$, were obtained by the corefinement of the Fe and Mn $K$-edge EXAFS data collected during DAFS measurements. Element-specific and site-specific EXAFS data, extracted from the DAFS spectra, were analyzed and fitted to standards' data generated using the multiple-scattering FEFF codes (Version 6.1) of Rehr *et al.*[13]

The real part of the Fourier transformed Fe and Mn EXAFS data and their best fit are presented in Fig. 1. A statistical $R$ factor of 0.032 was obtained. The best fit model structural parameters are presented in Table I. The lattice parameter was found to increase by about 1% relative to the bulk value of 8.5 Å.[14] The oxygen parameter $u$, which describes the position of O anions in the unit cell, increased by 3.2% relative to the bulk value of 0.38.[14] These results suggest a slight expansion in the unit cell in the Mn-ferrite film versus that of the bulk. The inversion parameter $\delta$ was calculated to be $18\% \pm 4\%$, a value consistent with the bulk value within the uncertainty of the analysis.

Site-specific structural parameters for Mn and Fe ions were obtained from fits of EXAFS data derived from DAFS

a)Electronic mail: fyang@ece.neu.edu.

 

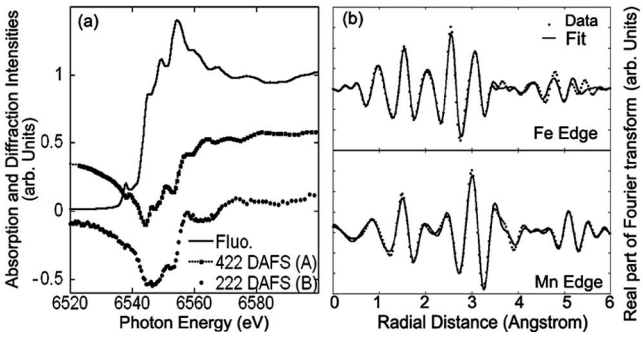


FIG. 1. (a) Mn *K* edge DAFS for the (422) and (222) Bragg reflections, together with EXAFS data. The scans are vertically shifted to allow comparison. (b) Fourier transformed Mn and Fe EXAFS data plotted with best fit data.

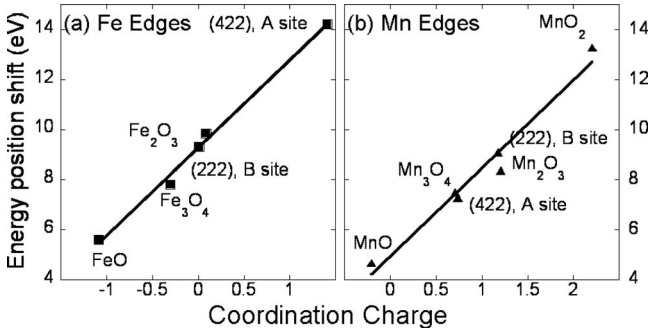


FIG. 2. Energy shift plotted as a function of coordination charge for various (a) Fe and (b) Mn oxide standards together with site-specific values for the Mn-ferrite films studied here [denoted by (hkl), A/B site].

spectra measured under (422) and (222) diffraction conditions. The results for site-specific bond disorder, i.e., Debye–Waller factors (DWFs), are listed in Table I. It is clear that DWFs are larger for octahedral sites than for tetrahedral sites, irrespective of cation species. The relatively high DWFs are indicative of octahedral structural disorder in these coordination shells.

Element-specific and site-specific cation distribution and oxidation state are essential information in correlating structure and magnetic properties of ferrites. Next, we focus on the near edge region of the anomalous diffraction and absorption spectra. The energy position of various near edge features correlate with the valence state of the transition metal ions. According to Kunzl's law,[15] the energy shifts, i.e., so-called chemical shifts, are found to vary linearly with the valence of the absorbing atom for a given ligand type. In our ferrite system, atoms residing on tetrahedral and octahedral sites have different numbers of surrounding ligands. Here, we apply the concept of "coordination charge,"[16] which we calculate using the Allred–Rochow electronegativities[17] following the method of Ovsyannikova *et al.*[18]

X-ray absorption near edge spectra, for standard Mn and Fe foils, and various Mn (i.e., MnO, $Mn_2O_3$, $MnO_2$, and $Mn_3O_4$) and Fe (i.e., FeO, $Fe_2O_3$, and $Fe_3O_4$) oxides, were collected and calibrated to reference metal foil spectra. The energy of the first x-ray absorption derivative peak was compared to that of the Fe and Mn foil spectra. The coordination charge varies linearly with the binding energy and chemical valence, and provides an estimate of the net charge of the absorbing transition metal ions. The energy positions of the absorption threshold for the cations in the $MnFe_2O_4$ film were determined with element and site specificity by the cusp position in the DAFS spectra, which corresponded with the first derivative peak of the DAFS-reduced EXAFS spectra. The coordination charges for Mn and Fe ions on different sites were calculated from these energy shifts and plotted with the reference oxides in Fig. 2. The coordination charges were then converted to oxidation states to allow for direct comparison. The results show that Mn and Fe ions on octahedral sites have a valence of +3.38(8) and +2.92(9), respectively, while Mn ions on tetrahedral sites have a +2.18(5) oxidation state. Even if one considers the possibility of reduced symmetry of Mn ions on octahedral sites, as suggested previously,[10] the corresponding valence would be +2.64(8). This confirms the presence of $Mn^{3+}$ ions on octahedral sites. The Jahn–Teller active $Mn^{3+}$ ions, having a $d^4$ electronic configuration, result in a distortion of the oxygen octahedra consistent with measured DWFs (Table I). The presence of $Mn^{3+}$ and its unquenched $d^4$ angular moment acts to increase the magnetic anisotropy and broaden the ferrimagnetic resonance linewidth.[19,20]

Knowledge of the site-specific valence state and cation distribution allows the calculation of thermomagnetization curves using molecular field theory (Fig. 3). In order to perform the fitting, an iterative refinement procedure was applied.[21] We begin with the molecular field coefficients for bulk $MnFe_2O_4$.[22,23] The film values of these coefficients were determined from a best fit to the thermomagnetization curves, reproducing the Néel temperature and the extrapolated 0 K saturation magnetization (Fig. 3). Based on the 0 K magnetization, the spin canting angle of the Mn on the *B* sublattice was determined to be 57°; slightly larger than the bulk value of 53°.[24] The molecular field coefficient $N_{abfm}$ accounts for the superexchange interaction between Mn and Fe ions on *A* and *B* sites. The film value was found to be 198

TABLE I. Structural properties determined from best fits of fluorescence EXAFS, and DAFS spectra measured at (422) and (222) Bragg peaks. The error bars in the least significant digit are given in parentheses.

| | Fluorescence EXAFS | Tetrahedral (422) DAFS | Octahedral (222) DAFS |
|---|---|---|---|
| Percentage of Fe at A sites | 9% | ··· | ··· |
| Percentage of Mn at B sites | 18(3)% | ··· | ··· |
| Lattice parameter *a* (Å) | 8.570(4) | ··· | ··· |
| Oxygen parameter *u* | 0.392(1) | ··· | ··· |
| Nearest neighbor (NN) DWF of Fe (Å$^2$) | 0.010(2) | 0.003 | 0.007(3) |
| Nearest neighbor (NN) DWF of Mn (Å$^2$) | 0.006(2) | 0.005(3) | 0.006(2) |
| Outer shell DWF of Fe (Å$^2$) | 0.010(2) | ··· | 0.006(3) |
| Outer shell DWF of Mn (Å$^2$) | 0.010(2) | 0.003(2) | 0.006(3) |

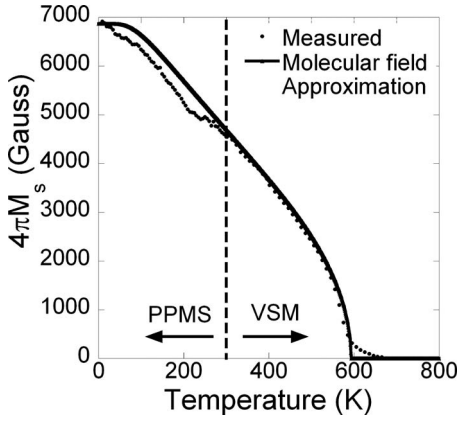


FIG. 3. Measured and calculated magnetization vs temperature data under an applied magnetic field of 5000 Oe. Calculation was based on molecular field theory.

compared with the bulk value of 187 $cm^3$/mole. $N_{AA}$ and $N_{BB}$ were determined to be −167.2 and −59.8, respectively. This represents a significant increase in the superexchange interaction. Molecular field simulations predict a room temperature magnetization that is 11% larger (4694 G) than the measured value of 4218 G. This result is consistent with the $Mn^{3+}$ ion-induced Jahn–Teller distortion, whose presence is evidenced by the relatively large DWF for Mn($B$)−O distances. We conjecture that this structural distortion increases the superexchange interaction, which contributes to an increase in Néel temperature and room temperature magnetization. The site-specific valence for the Mn and Fe cations correspond to a net charge of +8.31. These results indicate the existence of oxygen deficiencies, consistent with an underoxidation of cations due to the processing of films at low oxygen pressure. Oxygen defects may be another contributing factor to the large DWFs measured in the outer atomic shells of Mn and Fe ions.

This study exemplifies the utility of DAFS as a tool to determine element-specific and site-specific short-range order chemical, electronic, and structural properties. Such information is necessary to the understanding of magnetism in oxide systems.

Research was supported by the National Science Foundation and the Office of Naval Research and was performed, in part, at the National Synchrotron Light Source and the Advanced Photon Source, which are sponsored by the U.S. Department of Energy.

[1]X. Zuo, F. Yang, R. Mafhoum, R. Karim, A. Tebano, G. Balestrino, V. G. Harris, and C. Vittoria, IEEE Trans. Magn. **40**, 2811 (2004).
[2]A. Yang, Z. Chen, S. M. Islam, C. Vittoria, and V. G. Harris, J. Appl. Phys. **103**, 07E509 (2008).
[3]V. G. Harris, N. C. Koon, C. M. Williams, Q. Zhang, M. Abe, J. P. Kirkland, and D. A. Mckeown, IEEE Trans. Magn. **31**, 3473 (1995).
[4]V. G. Harris, N. C. Koon, C. M. Williams, Q. Zhang, M. Abe, and J. P. Kirkland, Appl. Phys. Lett. **68**, 2082 (1996).
[5]S. Calvin, E. E. Carpenter, V. G. Harris, and S. A. Morrison, Appl. Phys. Lett. **81**, 3828 (2002).
[6]S. Calvin, E. E. Carpenter, B. Ravel, V. G. Harris, and S. A. Morrison, Phys. Rev. B **66**, 224405 (2002).
[7]H. Stragier, J. O. Cross, J. J. Rehr, L. B. Sorensen, C. E. Bouldin, and J. C. Woicik, Phys. Rev. Lett. **69**, 3064 (1992).
[8]L. Sorensen, J. Cross, M. Newville, B. Ravel, J. Rehr, H. Stragier, C. Bouldin, and J. Woicik, in *Resonant Anomalous X-Ray Scattering: Theory and Applications*, edited by G. Materlik, C. Sparks, and K. Fischer (North-Holland, Amsterdam, 1994).
[9]I. J. Pickering, M. Sansone, J. Marsch, and G. N. George, J. Am. Ceram. Soc. **115**, 6302 (1993).
[10]E. Kravtsov, D. Haskel, A. Cady, A. Yang, C. Vittoria, X. Zuo, and V. G. Harris, Phys. Rev. B **74**, 104114 (2006).
[11]J. O. Cross, M. Newville, J. J. Rehr, L. B. Sorensen, C. E. Bouldin, G. Watson, T. Gouder, G. H. Lander, and M. I. Bell, Phys. Rev. B **58**, 11215 (1998).
[12]B. Ravel and M. Newville, J. Synchrotron Radiat. **12**, 537 (2005).
[13]J. J. Rehr, S. I. Zabinsky, and R. C. Albers, Phys. Rev. Lett. **81**, 3828 (2002).
[14]J. Smit and H. P. J. Wijn, *Ferrites* (Wiley, New York, 1959), p. 144.
[15]C. Mande and V. B. Sapre, in *Advances in X-Ray Spectroscopy*, edited by C. Bonnelle and C. Mande (Pergamon, New York, 1983), Chap. 17, p. 287.
[16]S. S. Batsanov, *Electronegativity of Elements and Chemical Bonds* (Izd. Sibirsk. Otd. Akad. Nauk SSSR, Novosibirsk, 1962) (in Russian).
[17]A. L. Allred and D. E. G. Rochow, J. Inorg. Nucl. Chem. **5**, 264 (1958).
[18]I. A. Ovsyannikova, S. S. Batsanov, L. I. Nasonova *et al.*, Bull. Acad. Sci. USSR, Phys. Ser. (Engl. Transl.) **31**, 936 (1967).
[19]P. Novak, V. Roskovec, Z. Simsa, and V. A. M. Brabers, J. Phys. (Paris), Colloq. **32**, C1 (1971).
[20]C. M. Williams, M. Abe, T. Itoh, and P. Lubitz, IEEE Trans. Magn. **30**, 4896 (1994).
[21]G. F. Dionne, J. Appl. Phys. **45**, 3621 (1974).
[22]G. F. Dionne, J. Appl. Phys. **63**, 3777 (1988).
[23]G. F. Dionne, J. Appl. Phys. **99**, 08M913 (2006).
[24]Z. Simsa and V. A. M. Brabers, IEEE Trans. Magn. **11**, 1303 (1975).